

P4.16 A CLOUD-RESOLVING SIMULATION OF TYPHOON RUSA (2002): POLYGONAL EYEWALL AND MESOVORTICES STRUCTURE

Wataru Mashiko *
Meteorological Research Institute, Tsukuba, Japan

1. INTRODUCTION

Due to the advance of observational technology, the detailed asymmetric structure in tropical cyclone cores is often captured. For examples, the visible images from a polar-orbiting satellite revealed a remarkable pentagonal eye pattern with mesovortices in Hurricane Isabel (2003) (Kossin and Schubert 2004). Understanding the details of inner structure of tropical cyclones is one of the most important issues because the inner-core structure near the eyewall is related not only to severe weather such as torrential rainfall and hazardous winds, but also to the change in the intensity of a tropical cyclone. The aim of this study is to show the successfully simulated mesovortices related to polygonal eyewall shape in Typhoon Rusa (2002) and to elucidate their structures and roles by using a three-dimensional cloud-resolving nonhydrostatic model. This presentation summarizes a recent study of Mashiko (2005) and shows the additional results.

2. RADAR OBSERVATION

Typhoon Rusa passed over the Amami Island in a mature stage with the central minimum pressure of 950 hPa at 12 UTC on 29 Aug. 2002. The operational JMA (Japan Meteorological Agency) radar located in Naze city on the Amami Island, denoted by \times in Fig. 1, captured the detailed eyewall structure. The distribution of precipitation intensity observed by Naze radar shows a large eye surrounded by the polygonal eyewall pattern with a radius of about 100 km (Fig. 1). Several straight line segments of band-shaped rainfall areas were often identified. The straight line segments were divided by several kinks in the eyewall. The remarkable kinks are shown with symbols of A-D in Fig. 1. An interesting feature is that rainfall was strong near the most of the kinks and on the azimuthally upwind side of kinks (C and D in Fig. 1), and the inner rainband extended outward from the kinks (C in Fig. 1).

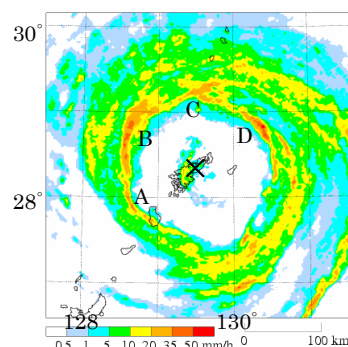


Fig. 1. Distribution of precipitation intensity observed by Naze radar at 1050 UTC on 29 Aug 2002. \times shows radar site. Alphabets (A-D) indicate the remarkable kinks of polygon.

3. NUMERICAL MODEL

Numerical experiment of Typhoon Rusa was conducted with a two-way triple-nested movable mesh Typhoon model (Mashiko and Muroi 2003). This model is based on Meteorological Research Institute/Numerical Prediction Division unified nonhydrostatic model of JMA. The horizontal grid spacing of the innermost domain is 2 km. For the model precipitation scheme, cold-rain explicit cloud microphysics is employed. The simulation is started at 12 UTC on 27 Aug. and run for 58 hours.

4. RESULTS

4.1 Characteristics of simulated polygonal eyewall

The simulated typhoon moved westward in comparison with the analyses, and the track error was about 250 km at $t=58$ h. The central minimum pressure had positive bias of about 12 hPa at the initial time, but it agreed with the analysis (950 hPa) in the later integration period (not shown). The simulated typhoon exhibited a pentagonal eyewall structure around $t=53$ h30m. The general features were reproduced successfully, although the simulated details differed somewhat from the radar analysis (Fig. 1), such as the number of kinks. Figures 2 show the vertically accumulated

* Corresponding author address: Wataru Mashiko,
Meteorological Research Institute,
1-1, Nagamine, Tsukuba 305-0052, Japan.
E-mail: wmashiko@mri-jma.go.jp.

hydrometeors (hereafter ACH) of cloud water, cloud ice, rainwater, snow and graupel, and the horizontal wind velocity at the lowest level of 20 m height $t=53\text{h}30\text{m}$. The sea surface pressure field is also shown with contours in Fig. 2. The straight line segments of ACH, especially inner edge of ACH, were divided by several kinks corresponding to those of sea surface pressure. They made a pentagonal-shaped eyewall that was distant about 100 km from the typhoon center. The distributions of ACH and upward motion (not shown) show that the convective activities in the eyewall were enhanced from the kinks to their azimuthally upwind side (except at the kink in the west). This feature is similar to that of the observed radar reflectivity, as shown in Fig. 1. The peak of the horizontal wind velocity was found near the kinks and it was about 20 % faster than the averaged azimuthal wind speed (Fig. 2b). The pentagonal pattern with these asymmetric features rotated anticlockwise around the center with a period of about 270 minutes. This speed of 39 m s^{-1} was slower than the lower tropospheric tangential wind speed in the eyewall ($\sim 50\text{ m s}^{-1}$).

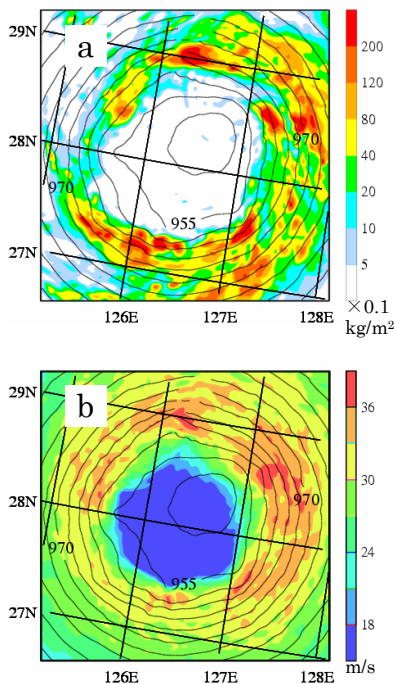


Fig. 2. (a) Vertically accumulated hydrometeors of cloud water, cloud ice, rainwater, snow and graupel, and (b) horizontal wind speed at a lowest level (20 m height) superposed by sea surface pressure with contour (interval; 3 hPa)

4.2 Structure of the simulated mesovortices

Figures 3 show the asymmetric pressure and the asymmetric horizontal wind fields at heights of 620 m and 5460 m at $t=53\text{h}30\text{m}$. To determine the storm center, a variational approach (Braun 2002) was used on the surface pressure field so that the azimuthal variance at all radii between the center and the outer portion (120 km) was minimized. The asymmetry around the eyewall was dominated by 5 meso-low pressure perturbations on the horizontal scale of 20-30 km below about a 4-km height. The meso-lows accompanied with cyclonic flow were located at the kinks of the pentagonal eyewall, and between them 5 meso-high pressure perturbations with anti-cyclonic flow existed below about a 1.5-km height. The maximum pressure deviation of meso-lows from the azimuthally averaged field was about 3 hPa, and that of the meso-highs was 1.5 hPa near the surface (Fig. 3a). The asymmetric structure in the inner area of the eyewall was dominated by wavenumber-1 pattern. The mesovortices structures within or near the eyewall were most predominant near the surface and tilted a little radially outward. The amplitude of the mesovortices weakened with height, and the wavenumber-1 pattern shifted to the upwind side of the azimuthal parent vortex flow dominated widely above a 4-km height. This vertical structure is similar to the observational results of Hurricane Olivia (1994), which revealed that the asymmetry in the inner core was dominated by an azimuthal wavenumber-2 feature below 3-km height and a wavenumber-1 feature above that height (Reasor et al. 2000).

The asymmetric wind fields produced the radial outflow between an upstream meso-high and a downstream meso-low, and the radial inflow between an upstream meso-low and a downstream meso-high around the eyewall. The maximum speed of these winds exceeded 10 m s^{-1} in the lower troposphere. They modulated the location of the eyewall, especially the radial outflow region in the southwest side (see Fig. 3a and Fig. 2a).

Besides, these radial flows modified by the mesovortices largely affected the convective activities in the eyewall. As indicated in section 4.1, strong convective activities were found mainly in the azimuthally upwind side of the kinks, which corresponded to the radial outflow region between an upstream

meso-high and a downstream meso-low. The area with the high equivalent potential temperature θ_e extended around the eyewall in the radial outflow region in the lower layer (Fig. 4). Vertical and radial cross sections of θ_e along the radial inflow (A-C in Fig. 3a) and outflow (C-B in Fig. 3a) are shown in Figs. 5a and 5b, respectively. The radial outflow was prominent inside the eyewall below a 2-km height, and it transported the high θ_e air (~ 371 K) from the eye into the eyewall (Fig. 5b). This transportation brought the strong convective activities in the eyewall. Meanwhile, in Fig. 5a the strong near-surface radial inflow reached into the inner eye, 70 km from the center. Consequently, the convective activities in the eyewall were not so strong.

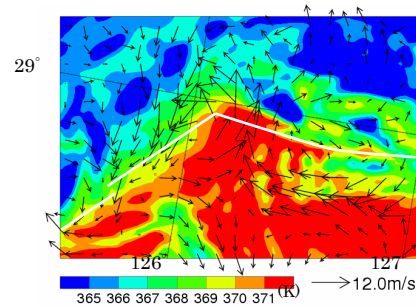


Fig. 4. Horizontal distribution of equivalent potential temperature with asymmetric winds at a height of 620 m in the square area of Fig. 3a. White solid lines denote the location of the upward motion in the eyewall at the same level.

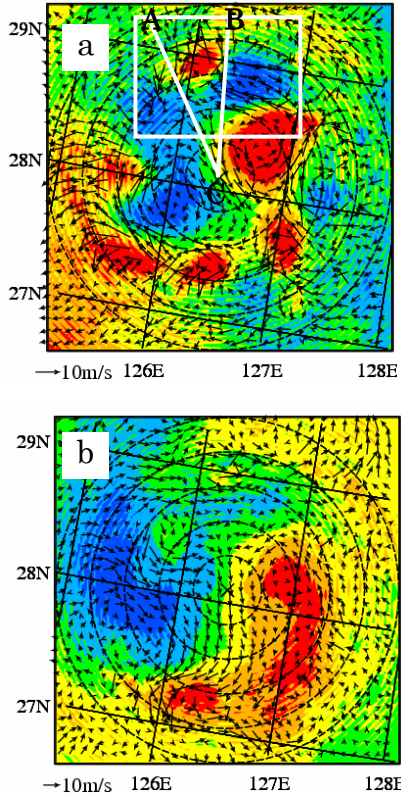


Fig. 3. Shaded in color is the asymmetric pressure field with the asymmetric winds relative to the moving cyclone at a height of (a) 620 m and (b) 5460 m after 53h30m of simulation. "x" shows the model typhoon center. The circles are placed at every 30 km from the center.

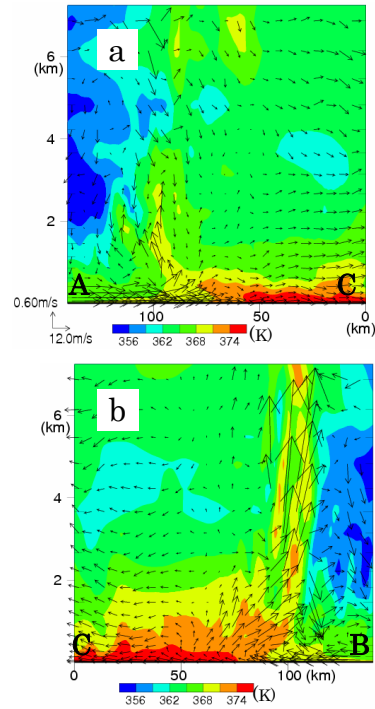


Fig. 5. Vertical cross sections of the simulated equivalent potential temperature superposed by typhoon-relative winds that are taken along (a) line A-C and (b) line C-B in Fig. 3a.

4.3 Motion of the minimum location and the geometric center of the pressure field

The location of the minimum sea surface pressure (Fig. 2) is related to one of the mesovortices shown in Fig. 3a. Figure. 6 illustrates the track of the minimum location and the geometric center decided in section

4.2 of the pressure field for 10.5 hours from $t=47h30m$ to $t=58h$. Since each of the mesovortices rotates anticlockwise around the geometric center the track of the minimum pressure location shows the trochoidal motion, while the track of the geometric center is also affected slightly by the wind the mesovortices (wavenumber-1 pattern) at about 5 km height modified around the geometric center.

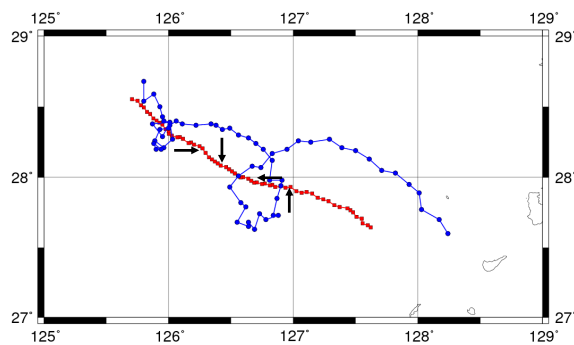


Fig. 6. The track of the minimum location (blue) and the geometric center (red) of the sea surface pressure field with 10 min. interval from $t=47h30m$ to $t=58h$. The arrows indicate the direction of the asymmetric winds relative to the moving cyclone at a height of 5460 m around the geometric center.

5. SUMMARY

In this study, the polygonal eyewall structure in Typhoon Rusa (2002) was examined by using a two-way triple-nested cloud-resolving nonhydrostatic model with a 2 km horizontal grid spacing on the finest nested mesh. The model successfully reproduced the features of the polygonal eyewall structure in the observed Rusa. The simulated asymmetric structure in the inner-core region was dominated by a number of mesovortices within or near the eyewall in the lower and middle troposphere. Meso-lows on the horizontal scale of 20-30 km were found at the kinks of polygonal eyewall, and between them meso-highs existed. The mesovortices affected not only the eyewall structure but also the convective activities in the eyewall and the typhoon motion.

REFERENCES

- Braun, S. A., 2002: A cloud-resolving simulation of Hurricane Bob (1991): Storm structure and eyewall buoyancy. *Mon. Wea. Rev.*, 130, 1573-1592.
- Kossin, J. P. and W. H. Schubert, 2004: Mesovortices in Hurricane Isabel. *Bull. Amer. Meteor. Soc.*, 85, 151-153.
- Mashiko, W. and C. Muroi, 2003: Development of a two-way multiply-nested movable mesh typhoon model using the cloud resolving nonhydrostatic model. *CAS/JSC WGNE Res. Activities in Atm. and Oceanic Modelling*, No.33, 5.22-5.23.
- Mashiko, W., 2005: Polygonal Eyewall and Mesovortices Structure in a Numerically Simulated Typhoon Rusa. *SOLA.*, 1, 29-32
- Reasor, P. D., M. T. Montgomery, F. D. Marks Jr. and J. F. Gamache, 2000: Low-wavenumber structure and evolution of the hurricane inner core observed by airborne dual-Doppler radar. *Mon. Wea. Rev.*, 128, 1653-1680.